Development 134, 1931-1941 (2007) doi:10.1242/dev.001891

Arabidopsis homologs of components of the SWR1 complex regulate flowering and plant development

Kyuha Choi[1], Chulmin Park[1], Jungeun Lee[1], Mijin Oh[1], Bosl Noh[2,3] and Ilha Lee[1,2,4,*]

The SWR1 complex (SWR1C) in yeast catalyzes the replacement of nucleosomal H2A with the H2AZ variant, which ensures full activation of underlying genes. We compared the phenotype of mutants in the homologs of SWR1C components in *Arabidopsis thaliana*. Mutations in *Arabidopsis SWC6* (*AtSWC6*), *SUPPRESSOR OF FRIGIDA 3* (*SUF3*) and *PHOTOPERIOD-INDEPENDENT EARLY FLOWERING 1* (*PIE1*), homologs of *SWC6*, *ARP6* and *SWR1*, respectively, caused similar developmental defects, including leaf serration, weak apical dominance, flowers with extra petals and early flowering by reduction in expression of *FLOWERING LOCUS C* (*FLC*), a strong floral repressor. Chromatin immunoprecipitation assays showed that AtSWC6 and SUF3 bind to the proximal region of the *FLC* promoter, and protoplast transfection assays showed that AtSWC6 colocalizes with SUF3. Protein interaction analyses suggested the formation of a complex between PIE1, SUF3, AtSWC6 and AtSWC2. In addition, H2AZ, a substrate of SWR1C, interacts with both PIE1 and AtSWC2. Finally, knockdown of the H2AZ genes by RNA interference or artificial microRNA caused a phenotype similar to that of *atswc6* or *suf3*. Our results strongly support the presence of an SWR1C-like complex in *Arabidopsis* that ensures proper development, including floral repression through full activation of *FLC*.

KEY WORDS: Flowering, Chromatin remodeling, SWR1 complex, FLC, AtARP6

INTRODUCTION

The development of eukaryotic organisms is controlled by dynamic and coordinated action of gene-specific transcription factors and chromatin modifiers (histone modification enzymes and ATP-dependent chromatin-remodeling enzymes) that establish and maintain spatial and temporal gene expression patterns (reviewed by Pole and Almouzni, 2006). In *Arabidopsis*, molecular genetic analyses have revealed many chromatin modifiers regulating the transition to flowering. Flowering time is regulated in *Arabidopsis* by a complex genetic network that consists of at least four interdependent genetic pathways, the long day, vernalization, gibberellin (GA) and autonomous pathways (reviewed by Putterill et al., 2004; Henderson and Dean, 2004). Among the genes involved in this complex genetic network, *FLOWERING LOCUS C* (*FLC*) is a central flowering regulator integrating the autonomous and vernalization pathways. *FLC* acts as a floral repressor, downregulating the expression of common downstream target genes – the so-called flowering pathway integrators *FT*, *SUPPRESSOR OF OVEREXPRESSION OF CO 1* (*SOC1*, *AGL20*) and *LEAFY* (Simpson and Dean, 2002). Ultimately, the expression level of these integrators determines the exact flowering time (Hepworth et al., 2002). Recently, the regulation of *FLC* through chromatin modifications has been intensively studied (reviewed by Lee, 2005).

Vernalization, a process accelerating flowering by sensing a long period of winter cold, suppresses the expression of *FLC* through a series of histone modifications, including deacetylation and the subsequent methylation of histone H3 at lysine 9 (K9) and lysine 27 (K27) (Sung and Amasino, 2004; Bastow et al., 2004). Deacetylation, and the subsequent K9 and K27 methylations, require *VERNALIZATION INSENSITIVE 3* (*VIN3*), which encodes a PHD-domain protein, and the methylations (particularly K9) require *VERNALIZATION 1* (*VRN1*) and *VRN2*, which encode a Myb-related DNA-binding protein and a Polycomb group protein homologous to *Drosophila Su[z]12*, respectively (Sung and Amasino, 2004; Bastow et al., 2004). After returning to warm temperature, the epigenetically repressed state of *FLC* is maintained by *LIKE HETEROCHROMATIN PROTEIN 1* (*LHP1*; also known as *TFL2* – TAIR), through the maintenance of the increased levels of H3K9 methylation at *FLC* chromatin (Sung et al., 2006).

In summer annuals lacking the strong *FLC* activator *FRIGIDA* (*FRI*), *FLC* expression is repressed by autonomous pathway genes. If any of them is mutated, *FLC* expression is increased resulting in late flowering (reviewed by Henderson and Dean, 2004; Lee, 2005). Among the autonomous pathway genes, *FVE* (*AtMSI4*), *FLOWERING LOCUS D* (*FLD*) and *RELATIVE OF EARLY FLOWERING 6* (*REF6*) are involved in histone modification at *FLC*. Mutation in any one of them causes hyperacetylation of H3 and H4 tails, resulting in upregulation of *FLC* (He et al., 2003; Ausin et al., 2004; Noh et al., 2004). *FVE* encodes a homolog of yeast MSI (multicopy suppressor of IRA1) and mammalian retinoblastoma-associated proteins RbAp46 and RbAp48 (also known as Rbbp7 and Rbbp4, respectively), which have a function in the histone deacetylase (HDAC) complex (Ausin et al., 2004; Kim et al., 2004). *FLD* encodes an amine oxidase, homologous to the human *LSD1* (lysine (K)-specific demethylase 1; also known as *AOF2* – Human Gene Nomenclature Database), whereas *REF6* encodes one of the plant jumonji-family proteins, the mammalian and yeast homologs of which function as histone demethylases (He et al., 2003; Shi et al., 2004; Noh et al., 2004; Tsukada et al., 2006). Thus, it is likely that *FLD* and *REF6* have roles in the deacetylation of *FLC* chromatin through histone demethylation.

[1]National Research Laboratory of Plant Developmental Genetics, Department of Biological Sciences, Seoul National University, Seoul, 151-742, Korea. [2]Global Research Laboratory for Flowering at SNU and UW, Seoul, 151-742, Korea. [3]Environmental Biotechnology National Core Research Center, Gyeongsang National University, Jinju 660-701, Korea. [4]Plant Metabolism Research Center, Kyung Hee University, Suwon 449-701, Korea.

*Author for correspondence (e-mail: ilhalee@snu.ac.kr)

Accepted 13 March 2007

It has also been reported that *Arabidopsis* homologs of components of the yeast PAF1 (RNA Polymerase Associated Factor 1) complex are required for trimethylation of H3 K4 at the promoter region of *FLC*, a hallmark of the active chromatin state (Krogan et al., 2003; Ng et al., 2003). Thus, mutation in any of the homologs of the PAF1 complex causes complete suppression of *FLC*, and consequently causes early flowering in winter annuals and autonomous pathway mutants (Oh et al., 2004; He et al., 2004). A similar suppression is observed in a mutation in *EARLY FLOWERING IN SHORT DAYS* (*EFS*), a homolog of the SET domain methyltransferase (Soppe et al., 1999; Kim et al., 2005). The *efs* mutation causes reduced trimethylation of H3 K4 or dimethylation of H3 K36 in *FLC* chromatin (Kim et al., 2005; Zhao et al., 2005).

It has also been reported that putative homologs of components of the ATP-dependent chromatin remodeling complexes are involved in the regulation of flowering time (reviewed by Reyes, 2006). In particular, several homologs of components of the yeast SWR1 complex (SWR1C), a member of the SWI2/SNF2 superfamily, have been reported to regulate *FLC* expression in *Arabidopsis*. The biochemical function of yeast SWR1C is to catalyze the replacement of H2A with its variant H2AZ (Mizuguchi et al., 2004; Kobor et al., 2004). H2AZ deposition by SWR1C is required for transcriptional regulation, heterochromatic barriers and genome stability in yeast (reviewed by Kamakaka and Biggins, 2005). For transcriptional regulation, the SWR1C deposits H2AZ into the transcriptional start site of a myriad of genes (Raisner et al., 2005; Zhang et al., 2005). Yeast SWR1C consists of 13 subunits and homologs of most of them exist in *Arabidopsis*, although SWC3 and SWC7 homologs have not been detected (see Table S1 in the supplementary material) (Meagher et al., 2005). The substrate of SWR1C, H2AZ, is also conserved in *Arabidopsis*: three homologs of H2AZ – HTA8 (At2g38810), HTA9 (At1g52740) and HTA11 (At3g54560) – are present (Yi et al., 2006). *PHOTOPERIOD-INDEPENDENT EARLY FLOWERING 1* (*PIE1*) is the *Arabidopsis* gene most homologous to *SWR1*, although it contains a SANT domain, which is usually found in ISWI family members (Noh and Amasino, 2003). Two other reported homologs of components of SWR1C are *ACTIN-RELATED PROTEIN 4* (*AtARP4*) and *SUPPRESSOR OF FRIGIDA 3* (*SUF3*; also known as *AtARP6* – TAIR) (Kandasamy et al., 2005; Choi et al., 2005; Deal et al., 2005; Martin-Trillo et al., 2006). The mutation in any of these homologs causes an early flowering phenotype through the reduction of *FLC* expression. Furthermore, the *pie1* and *suf3* mutants show similar developmental defects, including early flowering, leaf serration, production of extra petals and weak apical dominance.

To extend the study of SWR1C in *Arabidopsis*, we isolated a T-DNA insertion mutant in the homolog of *SWC6* (*AtSWC6*), another component of yeast SWR1C, and produced RNAi-mediated H2AZ gene-knockdown transgenic plants. The mutation in *AtSWC6* resulted in the same phenotypes as *suf3*. Chromatin immunoprecipitation assays showed that both AtSWC6 and SUF3 bind to the *FLC* promoter region. Consistently, when *SUF3:GFP* and *AtSWC6:RFP* constructs were co-transfected into protoplasts, complete colocalization of the two proteins was observed. In yeast two-hybrid and coimmunoprecipitation analyses, PIE1 interacted with SUF3, AtSWC6 and H2AZ, and AtSWC6 interacted with SUF3 and AtSWC2, another SWR1C component homolog. Finally, H2AZ gene-knockdown transgenic plants exhibited a similar phenotype to *atswc6*. Our results strongly suggest the presence of a homolog of SWR1C that regulates diverse aspects of plant development, including flowering.

MATERIALS AND METHODS

Plant materials and growth conditions

The *atswc6* mutant in a Col background was obtained from the *Arabidopsis* Stock Center (SAIL_1142/CS841940). For genetic analyses and construction of RNAi or amiRNA targeting H2AZs, we used the *Arabidopsis* Col:*FRI*^{SF2} strain (*FRI*) (Michaels and Amasino, 1999; Lee et al., 2000). All flowering-time mutant alleles used in this study have been described previously (Lee et al., 2000; Moon et al., 2005; Choi et al., 2005). Plants were grown as previously described (Choi et al., 2005). Flowering time was measured by counting the number of rosette leaves from at least 20 plants.

Plasmid construction

Primer pairs for amplification of cDNAs or genomic DNAs for plasmid construction are detailed in Table 1. To construct *AtSWC6* and *SUF3* overexpressors, full-length *AtSWC6* and *SUF3* cDNAs amplified by PCR were cloned into a binary vector myc-pBA (Zhou et al., 2005). For *35S-AtSWC6:GFP* construction, full-length *AtSWC6* cDNA without the stop codon was cloned into the modified pPZP211 (KH24) vector with the 35S promoter, GFP coding sequence, and NOS terminator derived from p326-GFP (Choi et al., 2005). For generation of *AtSWC6 p-AtSWC6:GUS* transgenic plants, 329 bp of upstream sequence from the stop codon of *At5g37060* (the neighboring gene) to the translational start site of *AtSWC6*, and the full-length genomic DNA of *AtSWC6* except for the stop codon, were amplified and cloned into the T-DNA binary vector pDW137 (Blázquez et al., 1997) as a translational fusion with the β-glucuronidase (*GUS*) gene. To prepare the construct expressing AtSWC6:GFP or AtSWC6:RFP fusion proteins for protoplast transient expression assays, the open reading frame of *AtSWC6* was cloned into p326-GFP and p326-RFP (Choi et al., 2005). For yeast two-hybrid assays, *AtSWC6*, *SUF3*, *AtSWC2* (*At2g36740*), *HTA8*, *HTA9*, *HTA11*, *PIE1-N* (1-1560 bp), *PIE1-M* (1560-3660 bp) and *PIE1-C* (3660-6168 bp) cDNAs were amplified and cloned into the *Bam*HI site or *Bgl*II site (for *AtSWC2*) of pGBKT7 and pGADT7 vectors, respectively. To produce the H2AZ RNAi construct, an inverted-repeat construct including the *HTA8*, *HTA9* and *HTA11* cDNAs was made using the pKANNIBAL vector in which a spliceable intron separates the two repeats (Helliwell and Waterhouse, 2003). Then, the region including the 35S promoter, two repeats, intron and OCS terminator was subcloned into the *Not*I site of the binary vector pART27 for transformation of *FRI*. Artificial miRNAs to specifically knockdown *HTA8*, *HTA9*, *HTA11*, and both *HTA9* and *HTA11*, were prepared by overlapping PCR using the pGEM-T Easy vector containing *MIR319a* as template (Schwab et al., 2006). PCR products including the amiRNA sequences were inserted into the binary vector pCGN18 (Choi et al., 2005). For *Agrobacterium*-mediated transient expression, the full-length *AtSWC2*, *HTA11* and *PIE1* cDNAs were cloned into myc-pBA or the modified pPZP211 (KH24).

Chromatin immunoprecipitation (ChIP) assay

Ten-day-old seedlings grown under long-day conditions were used for the ChIP assay as described previously (Kim et al., 2006). Polyclonal anti-myc (Santa Cruz Biotechnology, sc-789) was used for immunoprecipitation. PCR detection of *FLC* regions and *TUBULIN β-2* (*TUB2*) was performed with the primers shown in Table 1.

Analysis of gene expression

Total RNA was extracted from *Arabidopsis* using TRIZOL (Sigma). The digoxigenin (DIG) labeled-mRNA probes for *FLC*, *SOC1*, *SUF3* and *AtSWC6* were prepared as previously described (Choi et al., 2005). RNA blotting, hybridization and washes were performed as described in the DIG application manual (Roche). RT-PCR and primers for *SOC1*, *FLC*, *FT* and *TUB2* are as previously described (Lee et al., 2000; Moon et al., 2005). Primers for *AtSWC6*, *HTA8*, *HTA9* and *HTA11* are: *AtSWC6*, 5′-ATGGAGGAAGAGATGTCGAAC-3′ and 5′-CTATGCAACAAATTTCTGACA-3′; *HTA8*, 5′-ATGGCTGGTAAAGGTGGGAAAG-3′ and 5′-TCAATCCTTGGTGACTTTGTTG-3′; *HTA9*, 5′-ATGTCGGGGAAAGGGCTAAAG-3′ and 5′-CTATTCCTTGGCGGATTTGTTG-3′; *HTA11*, 5′-ATGGCAGGCAAAGGTGGAAAAG-3′ and 5′-TCACTCCTTGGTGGTTTTGTTG-3′.

Protein extraction and protein gel blotting

Plant tissues were harvested and ground in liquid nitrogen and solubilized in protein extraction buffer [10 mM HEPES pH 7.5, 100 mM NaCl, 1 mM EDTA, 0.2% (v/v) Triton X-100, 1 mM PMSF, and 1×protease inhibitor cocktail tablets (Roche)]. The debris was cleared by centrifugation at 15,000 ***g*** for 10 minutes at 4°C. Western blot analyses were performed to determine the myc:AtSWC6 or AtSWC6:GFP protein levels in *35S-myc:AtSWC6 atswc6* or *35S-AtSWC6:GFP atswc6* using anti-myc or anti-GFP antibodies.

Histochemical analysis of GUS activity

Detection of GUS expression in *AtSWC6p-AtSWC6:GUS* transgenic plants was performed according to Jefferson et al. (Jefferson et al., 1987). Plant samples were incubated in 90% acetone at room temperature for 10 minutes. The samples were rinsed once with staining solution without X-Gluc (0.2% Triton X-100, 50 mM sodium phosphate buffer pH 7.2, 2 mM potassium ferrocyanide, 2 mM potassium ferricyanide). The staining solution was replaced by staining solution containing 2 mM X-Gluc, and the plant samples were incubated overnight at 37°C. Samples were then observed after incubating in 50% ethanol at room temperature for 30 minutes.

Protoplast transient expression assay

Rosette leaves of Col plants grown for 4 weeks in long-day conditions were sampled for the isolation and transformation of protoplasts as described [Sheen, J. (2002). A transient expression assay using *Arabidopsis* mesophyll protoplasts. http://genetics.mgh.harvard.edu/sheenweb/]. Protoplasts were co-transformed with both GFP and RFP fusion constructs, totalling about 10 μg of plasmid DNA (prepared using the Qiagen Plasmid Maxi Kit) and cultured at 22°C in the dark. 12 hours after transformation, protoplasts were observed as previously described (Choi et al., 2005).

Yeast two-hybrid analysis and coimmunoprecipitation in tobacco transient expression system

The vectors and yeast strains (Matchmaker GAL4 Two-Hybrid System 3) were obtained from Clontech. The yeast two-hybrid assay was performed as previously described (Kim et al., 2006) and according to the manufacturer's instructions. Binary constructs presented in Table 1 were transiently expressed in *Nicotiana benthamiana* leaves and the coimmunoprecipitation assay performed as previously described (Kim et al., 2006).

RESULTS

Mutation in a homolog of *SWC6* causes the same developmental defects as *suf3*

The yeast ARP6 protein, a homolog of SUF3 in *Arabidopsis*, is a component of SWR1C, which consists of 13 subunits including SWR1 and SWC6/VSP71 (Kobor et al., 2004; Mizuguchi et al., 2004). Because there is a single homolog of SWC6, At5g37055, in *Arabidopsis*, we analyzed a T-DNA insertion mutant (SAIL_1142/CS841940) (Fig. 1). This mutant has a T-DNA insertion in the second intron of *At5g37055*, which results in the complete loss of expression (Fig. 1A-C). We named this gene *Arabidopsis thaliana SWC6* (*AtSWC6*). The *AtSWC6* gene encodes a HIT-type zinc-finger protein whose homologs, SWC6 and ZNHIT1, are subunits of the yeast SWR1 and mammalian SRCAP (SWI2/SNF2-related CBP activator protein) complexes, respectively (Cai et al., 2005; Mizuguchi et al., 2004). All three proteins have seven cysteines and one histidine highly conserved in a C-terminal region (see Fig. S1 in the supplementary material). The *atswc6* mutant showed an early flowering phenotype as well as leaf serration, flowers with extra petals, small siliques and weak apical dominance (Fig. 1D-H; Table 2; Table 3). When the *atswc6* mutation was introduced into *FRI*-containing Col (Col:*FRI*^{SF2}, referred to as *FRI* below) (Michaels and Amasino, 1999; Lee et al., 2000), which has very late flowering phenotype, the *atswc6* suppressed *FRI*-mediated late flowering (Fig. 1D,F; Table 3). The *atswc6 FRI* showed much earlier flowering than *FRI*, but similar flowering with

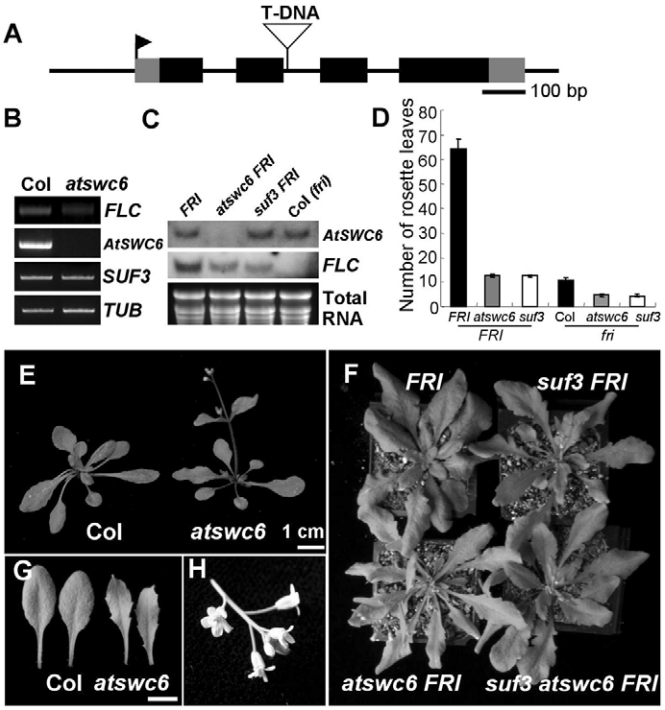

Fig. 1. Mutations in *AtSWC6* and *SUF3* cause the same phenotype. (**A**) Genomic structure of *AtSWC6* and T-DNA location in the *atswc6* mutant (SAIL_1142/CS841940). Black and gray boxes indicate exons and untranslated regions, respectively; lines between these boxes indicate introns; white triangle indicates T-DNA insertion; arrowhead indicates transcription start site. (**B**) RT-PCR analysis of *AtSWC6*, *FLC* and *SUF3* expression in wild type and *atswc6* mutant. RNA was extracted from 30-day-old *Arabidopsis* plants grown in long-day conditions. *TUBULIN* (*TUB*) was used as an internal control. (**C**) Northern blot analysis of *AtSWC6* and *FLC* expression. RNA was extracted from 10-day-old *FRI*, *atswc6 FRI*, *suf3 FRI* and Col. The *AtSWC6* transcript was not detected in the *atswc6* mutant, indicating that it is a null allele. (**D**) Flowering time of *FRI*, *atswc6 FRI* and *suf3 FRI* and of Col (*fri*), *atswc6 fri* and *suf3 fri* grown under long-day conditions. (**E**) Morphology of wild type (Col) and *atswc6* grown for 20 days under long-day conditions. (**F**) Morphology of *FRI*, *suf3 FRI*, *atswc6 FRI* and *suf3 atswc6 FRI* grown for 30 days under long-day conditions. (**G**) Leaf shape of wild type (Col) and *atswc6* mutant. (**H**) *atswc6* flower with five petals. Scale bars: in E and G, 1 cm.

Col. When *FLC* expression was checked, the *atswc6 FRI* line showed an approximately 50% reduction as compared with *FRI*, but fivefold higher expression than Col (Fig. 1C). Such a partial suppression of *FLC* was also observed in *suf3 FRI* (Fig. 1C) (Choi et al., 2005). Thus, the phenotypes caused by *atswc6* were almost identical to that of *suf3* reported previously (Choi et al., 2005). Consistently, the double mutant of *atswc6 suf3* was indistinguishable from any of the single mutants, irrespective of the presence of *FRI* (Fig. 1F). However, the expression analyses showed that the level of *SUF3* was not affected by *atswc6* and that of *AtSWC6* was not affected by *suf3*, indicating that the two genes do not regulate each other at the transcriptional level (Fig. 1B,C).

Phenotype of *AtSWC6* overexpression line and chromatin immunoprecipitation

To confirm whether the mutation of *At5g37055* is responsible for the *atswc6* phenotype, a full-length cDNA of *At5g37055* fused with 6 mycs or a GFP coding sequence driven by the 35S

Table 1. Primers used for plasmid construction in this study

Primer			Sequence
Overexpression line			
KH40	*35S-myc:POS*	F	5′-GGATCCGTATGGAGGAAGAGATGTCGAAC-3′
		R	5′-GGATCCCTATGCAACAAATTTCTGACA-3′
KH50	*35S-POS:GFP*	F	5′-GGATCCATGGAGGAAGAGATGTCGAAC-3′
		R	5′-GGATCCCTGCAACAAATTTCTGACAACG-3′
KH101	*35S-myc:SUF3*	F	5′-ATGCAGGATCCGTATGTCAAACATCGTTGTTCTA-3′
		R	5′-AACCCGGATCCTCAATGAAAGAATCGTCTACGAC-3′
For protoplast transient expression assay			
KH49	*POS:GFP*	F	5′-GGATCCATGGAGGAAGAGATGTCGAAC-3′
		R	5′-GGATCCCTGCAACAAATTTCTGACAACG-3′
KH59	*POS:RFP*	F	5′-GGATCCATGGAGGAAGAGATGTCGAAC-3′
		R	5′-GGATCCCCTGCAACAAATTTCTGACAACG-3′
For *POSp-POS:GUS pos* transgenic plant			
KH48	*POSp-POS:GUS*	F	5′-GGATCCTTATCTCCTTGGTCTCACTCT-3′
		R	5′-GGATCCCCTGCAACAAATTTCTGACAACG-3′
H2AZs RNAi			
KH85	HTA9 (*Xho*I-*Eco*RI)	F	5′-AATGCCTCGAGATGTCGGGGAAAGGTGCT-3′
		R	5′-AATGCGAATCCCTATTCCTTGGCGGATTT-3′
	HTA8 (*Eco*RI-*Kpn*I)	F	5′-AATGCGAATCCATGCTGGTAAAGGTGGG-3′
		R	5′-AATGCGGTACCTCAATCCTTGGTGACTTT-3′
	HTA11 (*Kpn*I-*Kpn*I)	F	5′-AATGCGGTACCATGGCAGGCAAAGGTGGA-3′
		R	5′-AATGCGGTACCTCACTCCTTGGTGGTTTTG-3′
	HTA9-8-11 (*Bam*HI-*Cla*I)	F	5′-AATGCGGATCCATGTCGGGGAAAGGTGCT-3′
		R	5′-AATGCATCGATTCACTCCTTGGTGGTTTTG-3′
amiR-HTA8, 9, 11, and both 9 and 11 (9&11)			
KH116	MIR319a	F	5′-ATAAACACACGCTCGGAC-3′
		R	5′-CATGGCGATGCCTTAAAT-3′
	A and B	A	5′-ATGCAGGATCCTAATACGACTCACTATAGGG-3′
		B	5′-ATGCAGGATCCAAGCTTATTTAGGTGACACTATAG-3′
KH117	amiR-HTA9	I	5′-gaTTGTCTTTAACAGACGATCCAtctctcttttgtattcc-3′
		II	5′-gaTGGATCGTCTGTTAAAGACAAtcaaagagaatcaatga-3′
		III	5′-gaTGAATCGTCTGTTCAAGACATtcacaggtcgtgatatg-3′
		IV	5′-gaATGTCTTGAACAGACGATTCAtctacatatatattcct-3′
KH118	amiR-HTA8	I	5′-gaTTGACGATGAATACGACCTACtctctcttttgtattcc-3′
		II	5′-gaGTAGGTCGTATTCATCGTCAAtcaaagagaatcaatga-3′
		III	5′-gaGTCGGTCGTATTCCTCGTCATtcacaggtcgtgatatg-3′
		IV	5′-gaATGACGAGGAATACGACCGACtctacatatatattcct-3′
KH119	amiR-HTA11	I	5′-gaTTAGCAGCCATCGTCTTGGCAtctctcttttgtattcc-3′
		II	5′-gaTGCCAAGACGATGGCTGCTAAtcaaagagaatcaatga-3′
		III	5′-gaTGACAAGACGATGCCTGCTATtcacaggtcgtgatatg-3′
		IV	5′-gaATAGCAGGCATCGTCTTGTCAtctacatatatattcct-3′
KH120	amiR-HTA9&11	I	5′-gaTTGTTGATGAGAGTCTTGTGGtctctcttttgtattcc-3′
		II	5′-gaCCACAAGACTCTCATCAACAAtcaaagagaatcaatga-3′
		III	5′-gaCCACAAGACTCTCCTCAACATtcacaggtcgtgatatg-3′
		IV	5′-gaATGTTGAGGAGAGTCTTGTGGtctacatatatattcct-3′
For yeast two-hybrid assay			
KH82	AD/BD-POS	F	5′-GGATCCGTATGGAGGAAGAGATGTCGAAC-3′
KH81		R	5′-GGATCCCTATGCAACAAATTTCTGACA-3′
MS32	AD/BD-SUF3	F	5′-AACCCGGATCCATATGTCAAACATCGTTGTTCTAGAC-3′
MS31		R	5′-AACCCGGATCCTCAATGAAAGAATCGTCTACGAC-3′
KH142	AD/BD-PIE1N	F	5′-ATGCGGATCCATATGGCGTCTAAAGGTGGTAAA-3′
KH141		R	5′-ATGCGGATCCATGGAGTATGTAAATCCAGTTGG-3′
KH144	AD/BD-PIE1M	F	5′-ATGCGGATCCATCCAACTGGATTTACATACTCC-3′
KH143		R	5′-ATGCGGATCCATGTTATCAAGCACACGCTTCTG-3′
KH146	AD/BD-PIE1C	F	5′-ATGCGGATCCATCAGAAGCGTGTGCTTGATAAC-3′
KH145		R	5′-ATGCGGATCCATCTACTCTATTTCTGAGATATC-3′
KH67	AD/BD-HTA9	F	5′-ATGCAGGATCCATATGTCGGGGAAAGGGCTAAAG-3′
KH64		R	5′-ATGCAGGATCCCTATTCCTTGGCGGATTTGTTG-3′
KH68	AD/BD-HTA8	F	5′-ATGCAGGATCCATATGGCTGGTAAAGGTGGGAAAG-3′
KH65		R	5′-ATGCAGGATCCTCAATCCTTGGTGACTTTGTTG-3′
KH69	AD/BD-HTA11	F	5′-ATGCAGGATCCATATGGCAGGCAAAGGTGGAAAAG-3′
KH66		R	5′-ATGCAGGATCCTCACTCCTTGGTGGTTTTGTTG-3′

Table 1 continued on next page.

Table 1. Continued

Primer			Sequence
For yeast two-hybrid assay			
KH104	AD/BD-AtSWC2	F	5′-ATATCTGTATGGAAATCGATGAAGAAGAG-3′
KH103		R	5′-ATATCTTTAATCTGAATCTTCTTCACT-3′
For chromatin immunoprecipitation assay			
	FLC-A	F	5′-AGTCTTAACTCGTGTCTTGCCA-3′
		R	5′-CATGAAGACAAGTGTTGTGGGAT-3′
	FLC-B	F	5′-TGTAGGCACGACTTTGGTAACACC-3′
		R	5′-GCAGAAAGAACCTCCACTCTACATC-3′
	FLC-C	F	5′-TATCTGGCCCGACGAAGAAA-3′
		R	5′-TTTGGGTTCAAGTCGCCGGAGATA-3′
	TUB2	F	5′-ACAAACACAGAGAGGAGTGAGCA-3′
		R	5′-ACGCATCTTCGGTTGGATGAGTGA-3′
	FLC-V	F	5′-CACACAACCTTTGTATCTTGTGTCT-3′
		R	5′-CATGAAGACAAGTGTTGTGGGAT-3′
For transient expression in tobacco			
KH17	*35S-SUF3:Flag*	F	5′-ATGCAGGATCCGTATGTCAAACATCGTTGTTCTA-3′
		R	5′-AACCCGGATCCAATGAAAGAATCGTCTACGAC-3′
KH146	*35S-HTA11:GFP*	F	5′-ATGCAGGATCCATGGCAGGCAAAGGTGGAAAA-3′
		R	5′-ATGCAGGATCCCATCCTTGGTGGTGGTTTTGTTGA-3′
KH27	*35S-PIE1:GFP*	F	5′-ATGCAGGATCCATGGCGTCTAAAGGTGGTAA-3′
		R	5′-ATGCAGGATCCACTCTATTTCTGAGATATCCG-3′
KH150	*35S-myc:AtSWC2*	F	5′-ATGCAGATCTGTATGGAAATCGATGAAGAAGAG-3′
		R	5′-ATGCAGATCTTATCTGAATCTTCTTCACT-3′

Restriction sites are underlined. Nucleotides in lowercase indicate the *MIR319a* sequence used in the overlapping PCR.
F, forward; R, reverse.

promoter was introduced into *atswc6* mutants. We generated four transgenic lines of *35S-myc:AtSWC6 atswc6* and 21 lines of *35S-AtSWC6:GFP atswc6* (Fig. 2). Western blot analysis showed the accumulation of myc:AtSWC6 and AtSWC6:GFP proteins in *35S-myc:AtSWC6 atswc6* and *35S-AtSWC6:GFP atswc6* (see Fig. S2 in the supplementary material), suggesting that the fusion proteins were functional. All *35S-myc:AtSWC6 atswc6* showed complete rescue, but *35S-AtSWC6:GFP atswc6* showed partial rescue of flowering phenotype (Fig. 2A-C; Table 3). The other phenotypes, such as serrated leaves, weak apical dominance and extra petals, were completely rescued in all of the transgenic lines (data not shown). It is noteworthy that overexpression of *AtSWC6* in *atswc6* did not cause an additional delay in flowering and showed the same expression levels of *FLC*, *FT* and *SOC1* as those of wild-type Col (Fig. 2C,D). Consistently, the *AtSWC6* overexpression lines in Col did not show any additional phenotype (data not shown).

Because the target of *SUF3* is *FLC* (Choi et al., 2005; Deal et al., 2005), we used chromatin immunoprecipitation (ChIP) to check whether AtSWC6 and SUF3 bind to the chromatin of the *FLC* promoter region. For this, we used *35S-myc:AtSWC6 atswc6* and *35S-myc:SUF3 suf3* transgenic lines showing complementation of the mutant phenotype (Fig. 2E). Both transgenic lines showed enrichment of AtSWC6 and SUF3 proteins at the proximal (FLC-B and FLC-C) region of the *FLC* promoter, but not at the distal (FLC-A) region of the promoter or first intron (FLC-V), suggesting that these proteins bind to the promoter region of *FLC* chromatin.

Expression patterns of *AtSWC6*

The expression of *AtSWC6* was examined by RT-PCR, northern blot analysis and histochemical GUS reporter assay in *AtSWC6p-AtSWC6:GUS* transgenic lines. *AtSWC6* transcripts were detected in all tissues tested at variable levels (Fig. 3A). *AtSWC6* expression was strongly detected at early stage, and increased slightly with developmental age (Fig. 3B,E). The level of *AtSWC6* transcripts did not show any daily rhythm, although that of *SUF3* increased at night (Fig. 3C). Furthermore, *AtSWC6* transcript levels were not affected by photoperiod or vernalization (Fig. 3D). In the transgenic plants expressing the translational fusion of *AtSWC6* genomic DNA with *GUS* (*AtSWC6p-AtSWC6:GUS*), GUS expression was detected strongly in actively dividing cells such as root and shoot apex, lateral root primordia, inflorescence, flowers, axillary bud, developing siliques and premature seeds (Fig. 3E). However, GUS expression was rarely detected in mature seeds and siliques, old leaves and stems (Fig. 3E).

To investigate whether *AtSWC6* expression is regulated by other flowering time genes, we examined the transcript level of *AtSWC6* in flowering-time mutants. The presence of *FRI* did not change the transcript level nor did an *flc* mutation (Fig. 1C; see Fig. S3 in the

Table 2. Comparison of morphological phenotype in *atswc6*

	Length of mature silique (mm)	Frequency (%) of extra petals	Number of cofluorescence
Col	14.2±1.05	0 (0/0/250)	3.4±0.63
atswc6	9.0±1.06	22.4 (4/52/194)	6.1±1.05
suf3	8.8±0.91	24.1 (5/54/191)	6.2±0.88

Sixty mature siliques from three plants per genotype were counted for measurement of the silique length. Two hundred and fifty flowers from each plant grown under long-day conditions were counted to assess the number of flowers with extra petals. The numbers in parentheses are the number of flowers with 6, 5 and 4 petals, respectively. For measurement of cofluorescence number, 25 plants were counted per genotype.

Table 3. Flowering time of *atswc6*, double mutants with *atswc6*, and transgenic plants

Genotype	No. of rosette leaves
Long days	
Col (*fri*)	10.9±0.74
atswc6	4.7±0.48
suf3	4.6±0.52
suf3 atswc6	4.5±0.53
flc	7.7±0.82
flc atswc6	3.9±0.74
fca	43.7±2.26
fca atswc6	11.5±2.01
ld	44.1±3.25
ld atswc6	11.8±1.48
ft	31.4±2.99
ft atswc6	17.8±3.19
ft suf3	17.4±2.67
FRI	63.6±3.69
atswc6 FRI	12.9±1.10
suf3 FRI	12.5±1.43
suf3 atswc6 FRI	12.8±1.87
35S-myc:AtSWC6 atswc6#1	11.0±0.76
35S-AtSWC6:GFP atswc6#1	9.1±0.96
Short days	
Col	62.3±3.83
suf3	16.1±2.66
atswc6	15.5±2.56
35S-myc:AtSWC6 atswc6#1	61.5±4.72
35S-AtSWC6:GFP atswc6#1	58.3±4.48

supplementary material). When we checked all the mutants involved in positive regulation of *FLC* (*suf4*, *vip4*, *pie1*, *suf3* and *abh1*), the autonomous pathway (*ld*, *fld*, *fve*, *fca*, *fy* and *fpa*), the photoperiod pathway (*gi* and *co*) and flowering pathway integrators (*ft* and *soc1*), the *AtSWC6* transcript level remained the same (see Fig. S3 in the supplementary material).

atswc6 mutation suppresses late flowering of autonomous pathway mutants and also causes early flowering independent of *FLC*

Double mutant analysis showed that the *atswc6* mutation reduced the *fca*- or *ld*-mediated high levels of *FLC* expression, thus resulting in earlier flowering and higher expression of *SOC1* (Fig. 4A,B,E). The *flc atswc6* double mutant flowered earlier than the *flc* single mutant, indicating that *AtSWC6* regulates other floral repressor(s) in addition to *FLC* (Fig. 4C). Additionally, *atswc6* partially suppressed late flowering of *ft* and caused upregulation of *SOC1*, which could be due to a decrease in *FLC* or in an additional repressor(s) or both in the *atswc6* mutant (Fig. 4D,F).

AtSWC6 and SUF3 colocalize in the nucleus of *Arabidopsis* protoplasts

To investigate the cellular localization of AtSWC6, we examined the florescence of GFP in the root of *35S-AtSWC6:GFP atswc6* transgenic plants. The AtSWC6:GFP proteins were localized in the nuclei of root cells (see Fig. S4 in the supplementary material). We also performed protoplast transient assays using constructs expressing AtSWC6:GFP, AtSWC6:RFP and SUF3:GFP fusion proteins under the control of the 35S promoter so as to compare in detail the localization of AtSWC6 and SUF3. Consistent with the localization of AtSWC6:GFP in roots, both AtSWC6:GFP and AtSWC6:RFP were localized in the nuclei of leaf protoplasts.

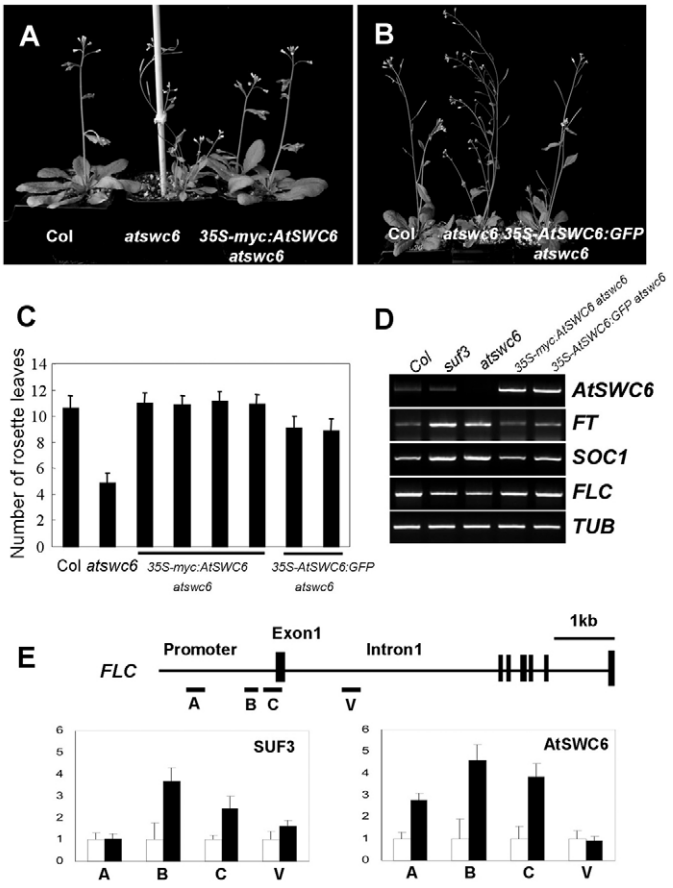

Fig. 2. Phenotype of *AtSWC6* overexpression line and chromatin immunoprecipitation. (**A**) Col, *atswc6* and *35S-myc:AtSWC6 atswc6* transgenic *Arabidopsis* plants grown for 35 days. (**B**) Col, *atswc6* and *35S-AtSWC6:GFP atswc6* transgenic plant grown for 35 days. (**C**) Number of rosette leaves at flowering of Col, *atswc6*, *35S-myc:AtSWC6 atswc6* and *35S-AtSWC6:GFP atswc6*. All plants in A-C were grown in long-day conditions. (**D**) Expression of *FT*, *SOC1* and *FLC* in Col, *suf3*, *atswc6*, *35S-myc:AtSWC6 atswc6* and *35S-AtSWC6:GFP atswc6* grown in short-day conditions for 4 weeks. Early flowering of *atswc6* and *suf3* is caused by the increased expression of the floral integrators *FT* and *SOC1*. (**E**) Col and *35S-myc:SUF3 suf3* (for SUF3 protein) or *35S-myc:AtSWC6 atswc6* (for AtSWC6 protein) transgenic seedlings grown under long-day conditions were used for ChIP assay using anti-myc antibody. Above is a map of the *FLC* gene showing the location of the regions examined in the *FLC* promoter (FLC-A for –1288 to –1470, FLC-B for –360 to –497, FLC-C for –45 to –164, relative to the ATG codon) and first intron (FLC-V for +1469–+1607). *TUB* was used as an internal control (white bars). The *x*-axis indicates relative enrichment.

When they were transfected simultaneously, the fluorescence overlapped entirely and the AtSWC6 proteins formed nuclear speckles (Fig. 5, upper panels). By contrast, when AtSWC6:RFP proteins were expressed with SUF3:GFP, most of the AtSWC6:RFP proteins moved to where SUF3:GFP proteins were localized, such that the fluorescence overlapped (Fig. 5, lower panels). Previously, it was reported that SUF3 is localized at the nuclear periphery (Choi et al., 2005). Our data thus indicate that AtSWC6:RFP relocates to the nuclear periphery where SUF3:GFP is localized, and strongly suggests that the two proteins interact.

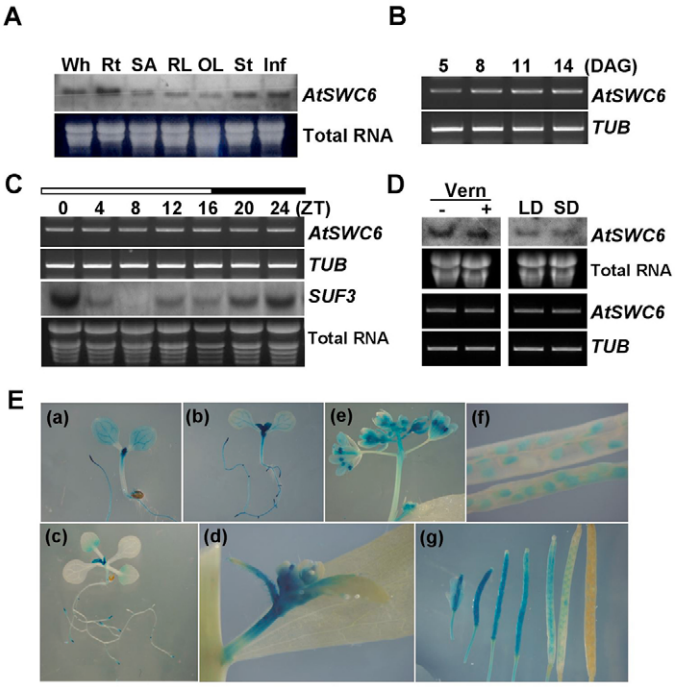

Fig. 3. Spatial and temporal expression of *AtSWC6*. (**A**) Northern blot analysis of *AtSWC6* expression in different *Arabidopsis* tissues. RNA was extracted from 20-day-old Col grown in long-day conditions for whole plants (Wh), root (Rt), shoot apex (SA) and rosette leaves (RL). RNA for old leaves (OL), stem (St) and inflorescence with flowers (Inf) was extracted from 40-day-old plants. (**B**) Temporal expression of *AtSWC6* assessed by RT-PCR. RNA was extracted from 5-, 8-, 11- and 14-day-old Col grown in long-day conditions. All the samples were harvested 4 hours after light on. (**C**) Diurnal rhythm of *AtSWC6* expression assessed by RT-PCR. RNA was extracted from 10-day-old Col grown in long-day conditions. Northern blot analysis with the same RNA showed diurnal rhythm in *SUF3* expression. (**D**) The effect of photoperiod and vernalization on *AtSWC6* expression. *FRI* with (+) and without (–) vernalization, and Col grown under long-day (LD) and short-day (SD) conditions were used for northern blot and RT-PCR analyses. For RT-PCR analysis, *TUB* expression served as an internal control. (**E**) Spatial expression patterns of *AtSWC6* were examined by GUS staining in the *AtSWC6p-AtSWC6:GUS* transgenic plant. Histochemical GUS staining was performed in whole (a) 3-, (b) 5- and (c) 10-day-old plants, in (d) inflorescence and flowers, (e) an axillary bud, (f,g) developing seeds and (g) siliques of different stages.

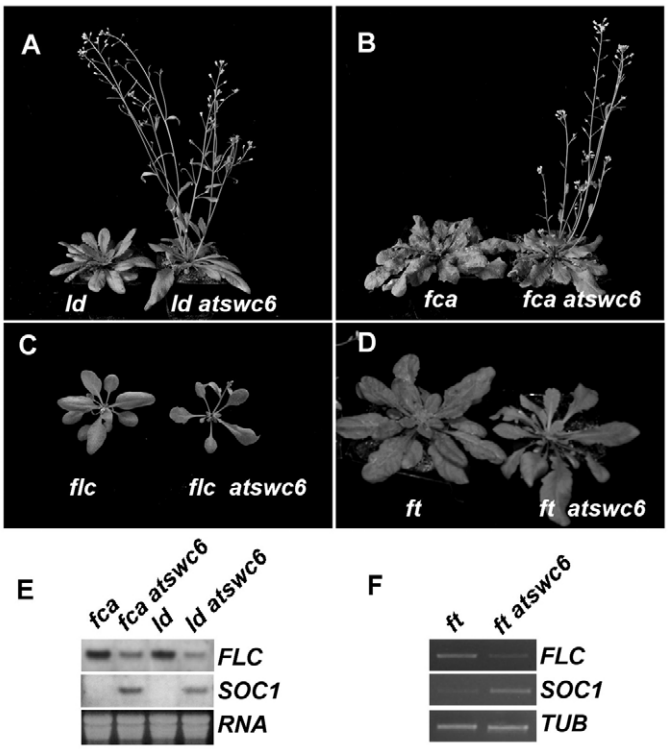

Fig. 4. Interaction of *atswc6* with other flowering-time mutants. Comparison of *Arabidopsis* flowering phenotype in (**A**) *ld-1* and *ld-1 atswc6*, (**B**) *fca-9* and *fca-9 atswc6*, (**C**) *flc-3* and *flc-3 atswc6*, (**D**) *ft-1* and *ft-1 atswc6*. Photographs were taken after 40 days in A and B, 20 days in C and 35 days in D. All plants were grown in long-day conditions. (**E**) Northern blot analysis of *FLC* and *SOC1* in single and double mutants. The transcript level of *FLC* was reduced by approximately half in double mutants (*fca-9 atswc6*, *ld-1 atswc6*) as compared with each single mutant. (**F**) RT-PCR analysis of *FLC* and *SOC1* in *ft-1* and *ft-1 atswc6*. *TUB* was used as an internal control. In E and F, RNA was extracted from 10-day-old plants grown in long day conditions.

Interactions among homologs of SWR1C components

We performed yeast two-hybrid assays to determine whether the *Arabidopsis* homologs of the yeast SWR1C components directly interact with each other. For this assay, we included three homologs of H2AZ – HTA8, HTA9 and HTA11 (Yi et al., 2006) – and a homolog of SWC2 (At2g36740), another component of SWR1C, which directly binds to H2AZ in yeast (Wu et al., 2005). The results showed that AtSWC6 interacts with SUF3 and AtSWC2, and revealed homodimerization of AtSWC6 (Fig. 6A). By contrast, SUF3 showed neither homodimerization nor interaction with AtSWC2, suggesting that AtSWC6 links SUF3 and AtSWC2. For PIE1 interaction analysis, we divided the PIE1 protein into three regions: an N-terminal region (PIE1-N, 1-520 aa) containing the HSA domain; a middle region (PIE1-M, 520-1220 aa) containing two ATPase domains; and a C-terminal region (PIE1-C, 1220-2055 aa) containing the putative SANT domain (Noh and Amasino, 2003). It has been suggested that the SANT domain is required for interaction with both HATs or HDACs and chromatin (Sterner et al., 2002; Noh and Amasino, 2003). PIE1-C interacted with both SUF3 and AtSWC6 but not with AtSWC2, and PIE1-N interacted with the three H2AZs (HTA8, HTA9, HTA11) but not with the other proteins tested (Fig. 6D,E). PIE1-M did not show any interaction, despite the fact that it contains ATPase domains. AtSWC2 also interacted with all three H2AZs (Fig. 6B,C). This suggests that AtSWC2 and PIE1-N together are involved in binding to H2AZ. To confirm the yeast two-hybrid result, we performed coimmunoprecipitation analysis using tobacco leaves transiently expressing myc:AtSWC6, AtSWC6:GFP, SUF3:Flag, myc:AtSWC2, HTA11:GFP and PIE1:GFP (Fig. 6F,G,H; see Fig. S6 in the supplementary material). The interactions of AtSWC6-SUF3, AtSWC6-AtSWC2, AtSWC2-HTA11, PIE1-SUF3, and PIE1-AtSWC6 were confirmed by the in planta coimmunoprecipitation assay. As expected, the negative control SUF4 failed to interact with AtSWC6 (Fig. 6G). Together, our results show interactions among PIE1, SUF3, AtSWC6, AtSWC2 and H2AZ.

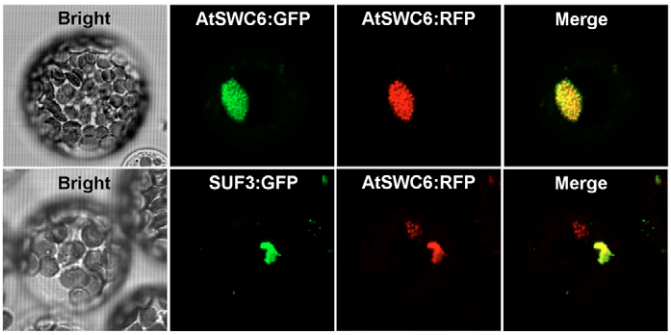

Fig. 5. AtSWC6 protein is colocalized with SUF3 in nucleus. Upper panels, *Arabidopsis* protoplast expressing AtSWC6-GFP and AtSWC6-RFP simultaneously. Lower panels, protoplast expressing SUF3-GFP and AtSWC6-RFP simultaneously. The right-most panels are merged images. The left-most panels show bright-field images of protoplasts.

Knockdown of H2AZ genes results in early flowering

To ascertain whether the knockdown of H2AZ genes would cause a similar phenotype to that observed in *pie1*, *atswc6*, and *suf3*. We generated RNAi-mediated knockdown transgenic plants targeting all three *Arabidopsis* H2AZ homologs (Fig. 7). Inverted repeats of the three tandemly fused H2AZ DNA fragments separated by a spliceable intron were inserted between the 35S promoter and the OCS terminator, and the construct was used for transformation of *FRI* (Fig. 7A). Among 62 T1 transformants, eight plants flowered with fewer than 30 rosette leaves, and 11 plants flowered with 30-40 rosette leaves. A total of 30 T1 plants (about 50%) flowered with fewer than 50 leaves, which is earlier flowering than *FRI* (Fig. 7B,C). We further analyzed three lines showing the early flowering phenotype (flowered with less than 35 leaves). RT-PCR analysis showed that the transcript levels of *HTA8* and *HTA11* were reduced by approximately 50%, and that of *HTA9* was slightly less reduced (Fig. 7D,E). Furthermore, RNA blot analysis showed that the early flowering lines had reduced *FLC* expression compared with *FRI*, suggesting that H2AZ is essential for full activation of *FLC* (Fig. 7D).

To confirm the requirement of individual H2AZ genes for high-level *FLC* expression, we generated artificial microRNA (amiR)-mediated knockdown transgenic plants specifically targeting mRNA of *HTA8* (*amiR-HTA8*), *HTA9* (*amiR-HTA9*) and *HTA11* (*amiR-HTA11*) in *FRI*, as previously described (Schwab et al., 2006). Although the targeted H2AZ was specifically knocked down, none of the *amiR-HTA8* and *HTA11* lines (48 and 64, respectively), and none (48 lines) of the *amiR-HTA9* lines except two, showed any obvious flowering phenotype, and the *FLC* expression level was the same as that of the *FRI* (Fig. 7F). However, two lines of *amiR-HTA9* showed earlier flowering (flowered with 38 and 40 leaves), and all *amiR-HTA9* lines showed some degree of leaf serration similar to that seen in *suf3* and *atswc6*.

When we checked the tissue specificity of each H2AZ, they were expressed in almost every tissue and there was no difference in the expression pattern between them, although *HTA9* showed higher expression than the other two (see Fig. S5 in the supplementary material). Thus, the absence of an obvious flowering phenotype in

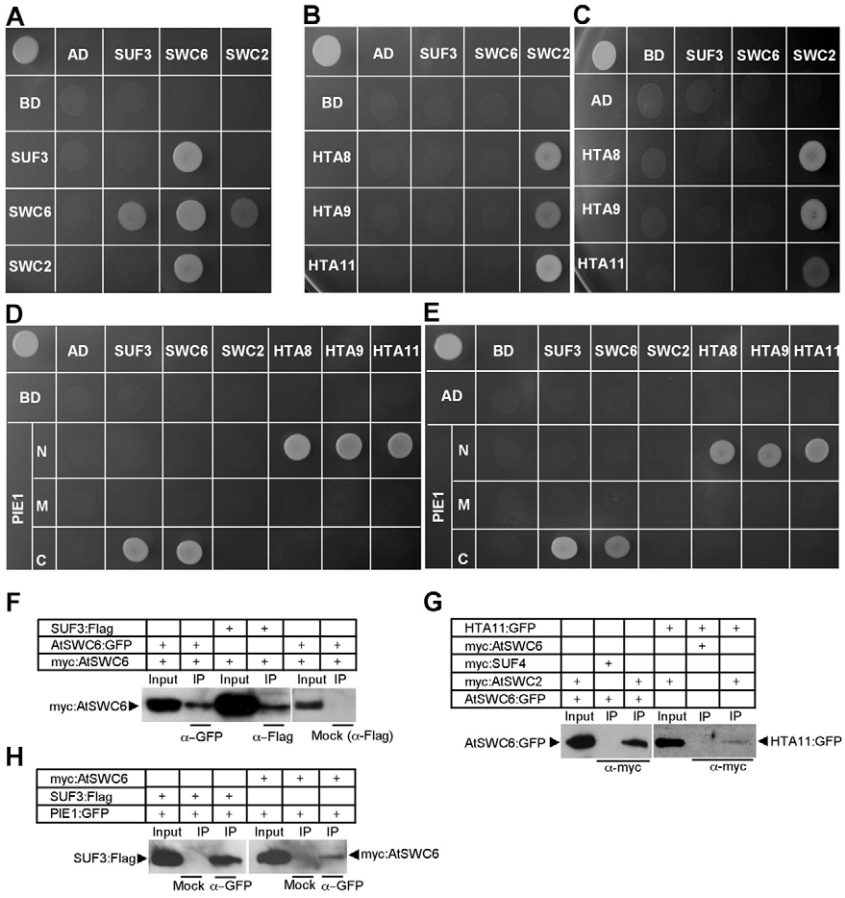

Fig. 6. *Arabidopsis* protein interactions analyzed by yeast two-hybrid and coimmunoprecipitation assays. (**A**) Interactions between SUF3, AtSWC6 and AtSWC2 (SWC2). (**B**) Interactions between SUF3, AtSWC6, AtSWC2 and HTA8, HTA9 and HTA11. (**C**) The same interaction analysis as B but with baits and preys changed. (**D**) Interaction between regions of PIE1 and SUF3, AtSWC6, AtSWC2, HTA8, HTA9 and HTA11. PIE1-N, PIE1-M and PIE1-C indicate PIE1 regions comprising amino acids 1-520, 520-1220 and 1220-2055, respectively. (**E**) The same interaction analysis as D but with baits and preys changed. (**F**) Protein gel blots showing interaction between AtSWC6 and SUF3. IP indicates immunoprecipitation of protein extracts from tobacco leaves transiently co-expressing epitope-tagged proteins, as listed above the blot, with anti-GFP (α-GFP) or anti-Flag (α-Flag) antibodies, as indicated below the blot. About 10% of the total sample used in each IP was loaded as an input control. Mock indicates IP with anti-Flag antibody. The immunoprecipitates and protein extracts were separated by 9% SDS-PAGE, transferred to polyvinylidene difluoride membranes, and probed with anti-myc antibody. (**G**) Protein gel blots showing interaction between AtSWC6, AtSWC2 and HTA11. Tobacco leaves co-expressing myc:SUF4 and AtSWC6:GFP were used as a negative control of IP. The protein blots were probed with anti-GFP antibody. (**H**) Protein gel blots showing interaction between PIE1 and SUF3 and AtSWC6. Mock indicates IP with no antibody. The protein blots were probed with anti-Flag (left) or anti-myc (right) antibodies.

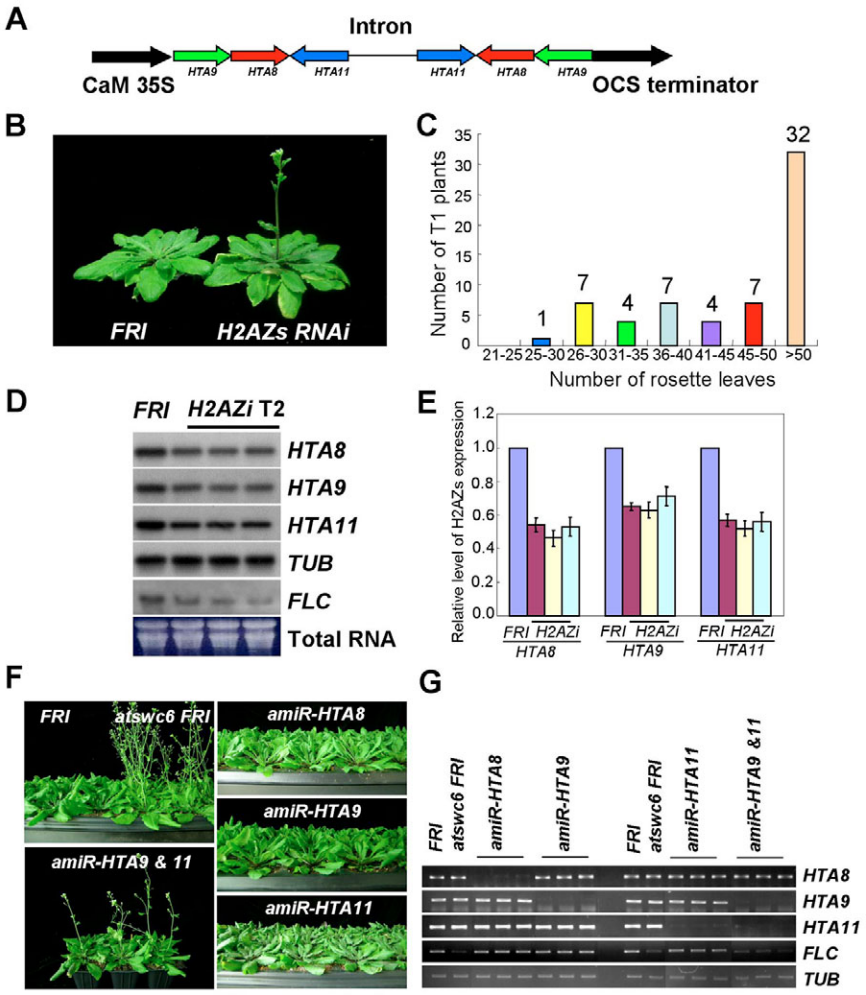

Fig. 7. Knockdown of H2AZ causes a similar phenotype to *atswc6*. (**A**) The RNAi construct targeting all three *Arabidopsis* H2AZ genes – *HTA8*, *HTA9* and *HTA11* (*AtH2AZs*). The tandemly fused *HTA8*, *HTA9* and *HTA11* cDNAs were arranged as inverted repeats which were separated by a spliceable intron. The construct was inserted between the CaMV 35S promoter and the OCS terminator. (**B**) *FRI* and *AtH2AZs RNAi* transgenic plants grown for 45 days under long-day conditions. (**C**) Distribution of flowering time in *AtH2AZs RNAi* T1 transformants. Plants were grown in long-day conditions. The number of plants in each category is given above each bar. (**D**) Expression of *HTA8*, *HTA9*, *HTA11* and *FLC* in three *AtH2AZs RNAi* lines that flowered with 35, 30 and 30 leaves. Homozygous lines were selected from the T2 generation of the three transgenic plants and RNA was extracted from 10-day-old plants grown in long-day conditions. All three *AtH2AZs RNAi* lines showed reduced expression of *HTA8*, *HTA9* and *HTA11*. The transcript level of *FLC* was also reduced. (**E**) The relative levels of *HTA8*, *HTA9* and *HTA11* transcripts in the three *AtH2AZs RNAi* lines as compared with *FRI* wild type. (**F**) *FRI*, *atswc6 FRI*, *amiR-HTA8*, *amiR-HTA9*, *amiR-HTA11* and *amiR-HTA9&11* T1 plants grown for 40 days after germination in long-day conditions. (**G**) RT-PCR analysis of expression of *HTA8*, *HTA9*, *HTA11* and *FLC* in *FRI*, *atswc6 FRI*, *amiR-HTA8*, *amiR-HTA9*, *amiR-HTA11* and *amiR-HTA9&11* T1 plants. RNA was extracted from leaves of T1 plants. *TUB* was used as an internal control.

the *amiR-HTA* lines is likely to be due to functional redundancy among the three H2AZs. To confirm this, we made *amiR-HTA9&11* transgenic lines that knocked down both *HTA9* and *HTA11* (Fig. 7G). These lines showed early flowering, reduced expression of *FLC*, leaf serration and flowers with extra petals (Fig. 7F). Among 32 transformants of the *amiR-HTA9&11*, 16 T1 plants flowered with 15-20 rosette leaves, which is similar to that of *suf3 FRI* or *atswc6 FRI*, and the rest also flowered before producing 30 rosettes. Taken together, our results strongly suggest that *HTA8*, *HTA9* and *HTA11* are functionally redundant and that *FLC* expression is regulated by the overall level of the three H2AZs.

DISCUSSION

Recently, the function of the ATP-dependent chromatin remodeling complex SWR1C has been intensively studied in yeast, a single-cell organism. The subunits of SWR1C, and of the mammalian homolog SRCAP, have been biochemically identified and analyzed (Kobor et al., 2004; Mizuguchi et al., 2004; Cai et al., 2005), but the presence of a homologous complex in plants has not been established. In addition, how SWR1C homologs affect development in higher eukaryotes remains largely unknown. Homologs of most SWR1C components are present in *Arabidopsis*, and thus the function of the relevant complex can be genetically dissected. In this work, we characterized AtSWC6 and analyzed its interaction with PIE1, SUF3 and AtSWC2, the homologs of components of SWR1C. We also analyzed the function of *Arabidopsis* H2AZ, a substrate of SWR1C. Our results strongly support the presence of an SWR1C-like complex in *Arabidopsis* that ensures proper development, including floral repression through full activation of *FLC*.

Homologs of SWR1C components in *Arabidopsis*

Mutations in three homologs of SWR1C components – *pie1*, *suf3* and *atswc6* – cause similar developmental defects (Noh and Amasino, 2003; Choi et al., 2005) (see also this study). All three mutants show leaf serration, weak apical dominance, flowers with extra petals, short siliques and early flowering. Genetically, all three mutants cause suppression of late flowering in autonomous pathway mutants as well as in an *FRI*-containing line. They also show earlier flowering than an *flc*-null and an approximately 50% reduction in *FLC* expression in an *FRI*-containing line. The *FLC* level in *suf3 FRI* or *atswc6 FRI* is fivefold higher than that in Col although the flowering time is similar, suggesting that *SUF3* and *AtSWC6* regulate additional floral repressor(s). In addition, the expression patterns of *SUF3*, *AtSWC6* and *PIE1* are similar (Fig. 3) (Noh and Amasino, 2003; Choi et al., 2005). Although all three genes are involved in the regulation of flowering time, their expression is affected neither by photoperiod nor vernalization, nor by any of the flowering-time mutants. It is notable, however, that *pie1* has a somewhat stronger effect than *suf3* or *atswc6* (Noh and Amasino, 2003). *pie1* also has the additional phenotypes of reduced fertility and short flowering stem in the Col background, phenotypes that were not obvious in *suf3* or *atswc6* in the same genetic background

(Noh and Amasino, 2003; Choi et al., 2005; Deal et al., 2005). Thus, *PIE1* might have a function that is at least partially independent from that of *SUF3* and *AtSWC6*.

In yeast, ARP6 and SWC6 are the most-tightly coupled components in SWR1C (Wu et al., 2005). They are necessary for the association with SWC2 and for nucleosome binding. Consistent with this, *SUF3* and *AtSWC6* have the most similar developmental function in *Arabidopsis*. The phenotypes of *suf3* and *atswc6* mutants are indistinguishable, and the *suf3 atswc6* double mutant has the same phenotype as each single mutant. The only difference we found between *SUF3* and *AtSWC6* was in the daily rhythm of expression; *SUF3*, but not *AtSWC6*, showed a daily rhythm, the significance of which is not clear because the *suf3* mutant does not show any conspicuous rhythmic defect. Together with the fact that overexpression of *SUF3* or *AtSWC6* does not cause any phenotype, our results strongly suggest that SUF3, AtSWC6 and PIE1 act together as a protein complex. The protein interaction analyses confirmed that the three proteins physically interact (Fig. 6).

Although we have not purified the SWR1C homolog, three lines of experimental evidence strongly support its presence in *Arabidopsis*. Firstly, protoplast transfection assays clearly showed that AtSWC6 and SUF3 are colocalized. AtSWC6 alone disperses throughout the nucleoplasm as speckles (Fig. 5). But when AtSWC6 and SUF3 are expressed together, AtSWC6 moves to the nuclear periphery where SUF3 is localized, as previously reported (Choi et al., 2005). Such a relocation of AtSWC6 strongly supports their interaction. In addition, the localization analyses may indicate that the nuclear periphery is the place where chromatin remodeling occurs, as previous reports suggested that gene activation or gene silencing occurs at the nuclear periphery (Misteli, 2004; Casolari et al., 2004). Consistent with this, both AtSWC6 and SUF3 bind to the proximal region of the *FLC* promoter in a ChIP assay. More direct evidence was provided by protein interaction analyses (Fig. 6), which showed that all of the putative components of the *Arabidopsis* SWR1C homolog are interconnected. Finally, when the expression of H2AZ was reduced to below a certain threshold level by RNAi or amiRNA, the plants showed similar developmental defects to those shown by *suf3*, *atswc6* and *pie1*, as expected (Fig. 7). Thus, although we have not directly measured the biochemical H2AZ replacement activity, our results strongly suggest that the complex including PIE1, SUF3 and AtSWC6 interacts with H2AZs biochemically and genetically.

The homolog of SWR1C is necessary for full activation of *FLC*

Genome-wide analyses in yeast showed that H2AZ is preferentially enriched at repressed promoters (Raisner et al., 2005; Zhang et al., 2005). However, H2AZ is more susceptible to loss from yeast chromatin upon increasing ionic strength, and the acetylated form of H2AZ is preferentially detected in active promoters (Zhang et al., 2005; Millar et al., 2006). Thus, it was proposed that H2AZ is deposited at repressed promoters and facilitates rapid activation, probably through acetylation of H2AZ by the NuA4 complex (Zhang et al., 2005; Millar et al., 2006). Consistent with this, H2AZ promotes full activation of target genes but does not impact upon repression. For example, the yeast deletion mutant of H2AZ shows approximately twofold attenuation in *YDC1* activation when induced by heat sock (Zhang et al., 2005). The deletion mutant also causes twofold reduction in *PHO5* and *GAL1* expression when induced by phosphate starvation and galactose treatment, respectively, but it always shows higher expression than the wild type before induction (Santisteban et al., 2000). We observed a similar result in the mutants of *Arabidopsis* homologs of SWR1C components. In the presence of *FRI*, *FLC* is strongly activated (Michaels and Amasino, 1999). However, if any of the SWR1C homologs are mutated, the expression of *FLC* is reduced twofold but is still higher than that in the plants without *FRI* (Fig. 1) (Noh and Amasino, 2003; Choi et al., 2005). Consistently, the knockdown lines of H2AZ showed a similar reduction (Fig. 7). Therefore, our results suggest that the SWR1C homolog in *Arabidopsis* promotes full activation of a target gene, *FLC*, as is proposed for the function of SWR1C in yeast.

Divergence of the SWR1C homolog in *Arabidopsis*

Histone variant H2AZ is highly conserved in a wide variety of species including yeast, *Tetrahymena*, *Drosophila*, chicken, *Xenopus*, mouse and human (reviewed by Kamakaka and Biggins, 2005). *Arabidopsis* also has three highly homologous H2AZs (Yi et al., 2006). H2AZ is essential for survival in *Tetrahymena*, *Drosophila* and mouse, but is not essential for yeast (Santisteban et al., 2000; Faast et al., 2001; Kamakaka and Biggins, 2005). Whether H2AZ is essential for survival of *Arabidopsis* is currently unknown owing to genetic redundancy. We also failed to knockdown all three H2AZ genes by RNAi, and thus it remains an open question. However, *suf3* and *atswc6* mutants are not embryo lethal, although *SUF3* and *AtSWC6* are single-copy genes in *Arabidopsis*. Because the homologs of SUF3 and AtSWC6 are found only in SWR1C and are not shared with other chromatin modification complexes, such as yeast INO80 or NuA4 or mammalian TRRAP/TIP60, this suggests that the SWR1C homolog in *Arabidopsis* is not essential for survival. It also indicates that the SWR1C homolog does not regulate the whole genome, but rather a certain group of genes that includes floral repressors.

The *Arabidopsis* homolog seems to be divergent from yeast SWR1C. Firstly, PIE1 is divergent from SWR1 in that it contains a SANT domain at the C-terminus, which is usually found in ISWI-family proteins (Noh and Amasino, 2003). Interestingly, AtSWC6 and SUF3 interact with the C-terminal region of PIE1 that contains the SANT domain (Fig. 6). By contrast, SWR1 interaction with SWC6 and ARP6 is dependent on the region between two ATPase domains (Wu et al., 2005), which corresponds to the middle region of PIE1 in our analysis. Secondly, SWC2 could not pull down SWC6 and ARP6 in a yeast *swr1* deletion mutant (Wu et al., 2005), but AtSWC2 directly interacts with AtSWC6, a SWC6 homolog, indicating that AtSWC2 is connected with AtSWC6 and SUF3 in *Arabidopsis*. Thirdly, the binding of H2AZ to the N-terminal region of SWR1 is not suggested in yeast, but in *Arabidopsis* H2AZ interacts with the N-terminal region of PIE1 and with AtSWC2. This therefore indicates the divergence of *Arabidopsis* and yeast SWR1C homologs. Further biochemical purification of the SWR1C homolog and functional studies using microarray and chromatin immunoprecipitation-coupled chip hybridization will help us to understand the crucial role of H2AZ and the SWR1C homolog in leaf and flower development and in flowering time control in *Arabidopsis*.

We thank ABRC for providing SAIL_1142/CS841940 seeds and R. Amasino for critical reading of the manuscript. This work was supported partially by the Korea Science and Engineering Foundation through the National Research Laboratory Program (No. M10600000164-06J0000-16410) and Global Research Laboratory Program (2006-03870), a grant from Seoul R&BD Program, and a grant from the Korea Science and Engineering Foundation through the Plant Metabolism Research Center, Kyung Hee University. K.C., C.P. and J.L. were supported by the Brain Korea 21 program.

Supplementary material

Supplementary material for this article is available at http://dev.biologists.org/cgi/content/full/134/10/1931/DC1

References

Ausin, I., Alonso-Blanco, C., Jarillo, J. A., Ruiz-Garcia, L. and Martinez-Zapater, J. M. (2004). Regulation of flowering time by FVE, a retinoblastoma-associated protein. *Nat. Genet.* **36**, 162-166.

Bastow, R., Mylne, J. S., Lister, C., Lippman, Z., Martienssen, R. A. and Dean, C. (2004). Vernalization requires epigenetic silencing of *FLC* by histone methylation. *Nature* **427**, 164-167.

Blázquez, M., Soowal, L., Lee, I. and Weigel, D. (1997). *LEAFY* expression and flower initiation in *Arabidopsis*. *Development* **124**, 3835-3844.

Cai, Y., Jin, J., Florens, L., Swanson, S. K., Kusch, T., Li, B., Workman, J. L., Washburn, M. P., Conaway, R. C. and Conaway, J. W. (2005). The mammalian YL1 protein is a shared subunit of the TRRAP/TIP60 histone acetyltransferase and SRCAP complexes. *J. Biol. Chem.* **280**, 13665-13670.

Casolari, J. M., Brown, C. R., Komili, S., West, J., Hieronymus, H. and Silver, P. A. (2004). Genome-wide localization of the nuclear transport machinery couples transcriptional status and nuclear organization. *Cell* **117**, 427-439.

Choi, K., Kim, S., Kim, S. Y., Kim, M., Hyun, Y., Lee, H., Choe, S., Kim, S. G., Michaels, S. and Lee, I. (2005). *SUPPRESSOR OF FRIGIDA3* encodes a nuclear ACTIN-RELATED PROTEIN6 required for floral repression in *Arabidopsis*. *Plant Cell* **17**, 2647-2660.

Deal, R. B., Kandasamy, M. K., McKinney, E. C. and Meagher, R. B. (2005). The nuclear actin-related protein ARP6 is a pleiotropic developmental regulator required for the maintenance of *FLOWERING LOCUS C* expression and repression of flowering in *Arabidopsis*. *Plant Cell* **17**, 2633-2646.

Faast, R., Thonglairoam, V., Schulz, T. C., Beall, J., Wells, J. R., Taylor, H., Matthaei, K., Rathjen, P. D., Tremethick, D. J. and Lyons, I. (2001). Histone variant H2A.Z is required for early mammalian development. *Curr. Biol.* **11**, 1183-1187.

He, Y., Michaels, S. D. and Amasino, R. M. (2003). Regulation of flowering time by histone acetylation in *Arabidopsis*. *Science* **302**, 1751-1754.

He, Y., Doyle, M. R. and Amasino, R. M. (2004). PAF1-complex-mediated histone methylation of *FLOWERING LOCUS C* chromatin is required for the vernalization-responsive, winter-annual habit in *Arabidopsis*. *Genes Dev.* **18**, 2774-2784.

Helliwell, C. and Waterhouse, P. (2003). Constructs and methods for high-throughput gene silencing in plants. *Methods* **30**, 289-295.

Henderson, I. R. and Dean, C. (2004). Control of *Arabidopsis* flowering: the chill before the bloom. *Development* **131**, 3829-3838.

Hepworth, S. R., Valverde, F., Ravenscroft, D., Mouradov, A. and Coupland, G. (2002). Antagonistic regulation of flowering-time gene *SOC1* by CONSTANS and FLC via separate promoter motifs. *EMBO J.* **21**, 4327-4337.

Jefferson, R. A., Kavanagh, T. A. and Bevan, M. W. (1987). GUS fusions: β-Glucuronidase as a sensitive and versatile gene fusion marker in higher plants. *EMBO J.* **6**, 3901-3907.

Kamakaka, R. T. and Biggins, S. (2005). Histone variants: deviants? *Genes Dev.* **19**, 295-310.

Kandasamy, M. K., Deal, R. B., McKinney, E. C. and Meagher, R. B. (2005). Silencing the nuclear actin-related protein AtARP4 in *Arabidopsis* has multiple effects on plant development, including early flowering and delayed floral senescence. *Plant J.* **41**, 845-858.

Kim, H. J., Hyun, Y., Park, J. Y., Park, M. J., Park, M. K., Kim, M. D., Kim, H. J., Lee, M. H., Moon, J., Lee, I. et al. (2004). A genetic link between cold responses and flowering time through FVE in *Arabidopsis thaliana*. *Nat. Genet.* **36**, 167-171.

Kim, S. Y., He, Y., Jacob, Y., Noh, Y. S., Michaels, S. and Amasino, R. (2005). Establishment of the vernalization-responsive, winter-annual habit in *Arabidopsis* requires a putative histone H3 methyl transferase. *Plant Cell* **17**, 3301-3310.

Kim, S., Choi, K., Park, C., Hwang, H.-J. and Lee, I. (2006). *SUPPRESSOR OF FRIGIDA4* encoding a C2H2 type zinc finger protein represses flowering by transcriptional activation of *Arabidopsis FLOWERING LOCUS C*. *Plant Cell* **18**, 2985-2998.

Kobor, M. S., Venkatasubrahmanyam, S., Meneghini, M. D., Gin, J. W., Jennings, J. L., Link, A. J., Madhani, H. D. and Rine, J. (2004). A protein complex containing the conserved Swi2/Snf2-related ATPase Swr1p deposits histone variant H2A.Z into euchromatin. *PLoS Biol.* **2**, 0587-0599.

Krogan, N. J., Dover, J., Wood, A., Schneider, J., Heidt, J., Boateng, M. A., Dean, K., Ryan, O. W., Golshani, A., Johnston, M. et al. (2003). The Paf1 complex is required for histone H3 methylation by COMPASS and Dot1p: linking transcriptional elongation to histone methylation. *Mol. Cell* **11**, 721-729.

Lee, H., Suh, S. S., Park, E., Cho, E., Ahn, J. H., Kim, S. G., Lee, J. S., Kwon, Y. M. and Lee, I. (2000). The AGAMOUS-LIKE 20 MADS domain protein integrates floral inductive pathways in Arabidopsis. *Genes Dev.* **14**, 2366-2376.

Lee, I. (2005). Multiple regulatory mechanisms of the floral repressor *FLC*, a gene conferring a vernalization requirement in *Arabidopsis*. *Flowering Newsl.* **40**, 52-59.

Martin-Trillo, M., Lazaro, A., Poethig, R. S., Gomez-Mena, C., Pineiro, M. A., Martinez-Zapater, J. M. and Jarillo, J. A. (2006). *EARLY IN SHORT DAYS 1* (*ESD1*) encodes ACTIN-RELATED PROTEIN 6 (AtARP6), a putative component of chromatin remodelling complexes that positively regulates FLC accumulation in *Arabidopsis*. *Development* **133**, 1241-1252.

Meagher, R. B., Deal, R. B., Kandasamy, M. K. and McKinney, E. C. (2005). Nuclear actin-related proteins as epigenetic regulators of development. *Plant Physiol.* **139**, 1576-1585.

Michaels, S. D. and Amasino, R. M. (1999). *FLOWERING LOCUS C* encodes a novel MADS domain protein that acts as a repressor of flowering. *Plant Cell* **11**, 949-956.

Millar, C. B., Xu, F., Zhang, K. and Grunstein, M. (2006). Acetylation of H2AZ Lys 14 is associated with genome-wide gene activity in yeast. *Genes Dev.* **20**, 711-722.

Misteli, T. (2004). Spatial positioning; a new dimension in genome function. *Cell* **119**, 153-156.

Mizuguchi, G., Shen, X., Landry, J., Wu, W. H., Sen, S. and Wu, C. (2004). ATP-driven exchange of histone H2AZ variant catalyzed by SWR1 chromatin remodeling complex. *Science* **303**, 343-348.

Moon, J., Lee, H., Kim, M. and Lee, I. (2005). Analysis of flowering pathway integrators in *Arabidopsis*. *Plant Cell Physiol.* **46**, 292-299.

Ng, H. H., Robert, F., Young, R. A. and Struhl, K. (2003). Targeted recruitment of Set1 histone methylase by elongating Pol II provides a localized mark and memory of recent transcriptional activity. *Mol. Cell* **11**, 709-719.

Noh, B., Lee, S. H., Kim, H. J., Yi, G., Shin, E. A., Lee, M., Jung, K. J., Doyle, M. R., Amasino, R. M. and Noh, Y. S. (2004). Divergent roles of a pair of homologous jumonji/zinc-finger-class transcription factor proteins in the regulation of *Arabidopsis* flowering time. *Plant Cell* **16**, 2601-2613.

Noh, Y. S. and Amasino, R. M. (2003). *PIE1*, an ISWI family gene, is required for FLC activation and floral repression in *Arabidopsis*. *Plant Cell* **15**, 1671-1682.

Oh, S., Zhang, H., Ludwig, P. and van Nocker, S. (2004). A mechanism related to the yeast transcriptional regulator Paf1c is required for expression of the *Arabidopsis FLC/MAF* MADS box gene family. *Plant Cell* **16**, 2940-2953.

Pole, S. E. and Almouzni, G. (2006). Chromatin assembly: a basic recipe with various flavours. *Curr. Opin. Genet. Dev.* **16**, 104-111.

Putterill, J., Laurie, R. and Macknight, R. (2004). It's time to flower: the genetic control of flowering time. *BioEssays* **26**, 363-373.

Raisner, R. M., Hartley, P. D., Meneghini, M. D., Bao, M. Z., Liu, C. L., Schreiber, S. L., Rando, O. J. and Madhani, H. D. (2005). Histone variant H2A.Z marks the 5′ ends of both active and inactive genes in euchromatin. *Cell* **123**, 233-248.

Reyes, J. C. (2006). Chromatin modifiers that control plant development. *Curr. Opin. Plant Biol.* **9**, 21-27.

Santisteban, M. S., Kalashnikova, T. and Smith, M. M. (2000). Histone H2A.Z regulates transcription and is partially redundant with nucleosome remodeling complexes. *Cell* **103**, 411-422.

Schwab, R., Ossowski, S., Riester, M., Warthmann, N. and Weigel, D. (2006). Highly specific gene silencing by artificial microRNAs in *Arabidopsis*. *Plant Cell* **18**, 1121-1133.

Shi, Y., Lan, F., Matson, C., Mulligan, P., Whetstine, J. R., Cole, P. A., Casero, R. A. and Shi, Y. (2004). Histone demethylation mediated by the nuclear amine oxidase homolog LSD1. *Cell* **119**, 941-953.

Simpson, G. G. and Dean, C. (2002). *Arabidopsis*, the Rosetta stone of flowering time? *Science* **296**, 285-289.

Soppe, W. J., Bentsink, L. and Koornneef, M. (1999). The early-flowering mutant *efs* is involved in the autonomous promotion pathway of *Arabidopsis thaliana*. *Development* **126**, 4763-4770.

Sterner, D. E., Wang, X., Bloom, M. H., Simon, G. M. and Berger, S. L. (2002). The SANT domain of Ada2 is required for normal acetylation of histone by the yeast SAGA complex. *J. Biol. Chem.* **277**, 8178-8186.

Sung, S. and Amasino, R. M. (2004). Vernalization in *Arabidopsis thaliana* is mediated by the PHD finger protein VIN3. *Nature* **427**, 159-164.

Sung, S., He, Y., Eshoo, T., Tamada, Y., Johnson, L., Nakahigashi, K., Goto, K., Jacobsen, S. E. and Amasino, R. M. (2006). Epigenetic maintenance of the vernalized state in *Arabidopsis thaliana* requires LIKE HETEROCHROMATIN PROTEIN 1. *Nat. Genet.* **38**, 706-710.

Tsukada, Y., Fang, J., Erdjument-Bromage, H., Warren, M. E., Borchers, C. H., Tempst, P. and Zhang, Y. (2006). Histone demethylation by a family of JmjC domain-containing proteins. *Nature* **439**, 811-816.

Wu, W. H., Alami, S., Luk, E., Wu, C. H., Sen, S., Mizuguchi, G., Wei, D. and Wu, C. (2005). Swc2 is a widely conserved H2AZ-binding module essential for ATP-dependent histone exchange. *Nat. Struct. Mol. Biol.* **12**, 1064-1071.

Yi, H., Sardesai, N., Fujinuma, T., Chan, C. W., Veena and Gelvin, S. B. (2006). Constitutive expression exposes functional redundancy between the *Arabidopsis* histone H2A gene *HTA1* and other H2A gene family members. *Plant Cell* **18**, 1575-1589.

Zhang, H., Roberts, D. N. and Cairns, B. R. (2005). Genome-wide dynamics of Htz1, a histone H2A variant that poises repressed/basal promoters for activation through histone loss. *Cell* **123**, 219-231.

Zhao, Z., Yu, Y., Meyer, D., Wu, C. and Shen, W. H. (2005). Prevention of early flowering by expression of *FLOWERING LOCUS C* requires methylation of histone H3 K36. *Nat. Cell Biol.* **7**, 1256-1260.

Zhou, Q., Hare, P. D., Yang, S. W., Zeidler, M., Huang, L. F. and Chua, N. H. (2005). FHL is required for full phytochrome A signaling and shares overlapping functions with FHY1. *Plant J.* **43**, 356-370.